International Journal of Thermodynamics (IJoT)
ISSN 1301-9724 / e-ISSN 2146-1511
https://dergipark.org.tr/en/pub/ijot

Vol. 29 (No. 1), pp. 061-068, 2026
doi: 10.5541/ijot.1807337
Published online: March 1, 2026

Research Article

OTEC-Assisted Mariculture Integrated with Symbiotic Anemone–Zooxanthellae Systems: A Numerical Investigation for Sustainable Coastal Applications

[1]* M. Ökten

[1] Manisa Celal Bayar University, Hasan Ferdi Turgutlu Faculty of Technology, Department of Energy Systems Engineering, Manisa, 45400, Turkiye
E-mail: [1]*mert.okten@cbu.edu.tr

Received 20 October 2025, Revised 05 December 2025, Accepted 10 February 2026

Abstract

Coastal regions are under pressure globally due to the complex balance between increasing energy demand, food production, and environmental sustainability. This study presents a numerical model and feasibility analysis of an integrated system that aims to simultaneously reduce the environmental impacts of energy production and marine aquaculture. The proposed model creates a multifunctional circular production concept by combining an Ocean Thermal Energy Conversion (OTEC) system with a fish farming unit and a symbiotic anemone–zooxanthellae-based bioremediation module. The model was developed for the conditions of Turkiye's southeastern Aegean coastline and simulates base load energy production via the Organic Rankine Cycle (ORC) even at low temperature differences, as well as the removal of inorganic nutrients (ammonia, nitrate) from fish farms by the symbiotic system and the release of photosynthetic oxygen into the environment during this process. Based on advection–diffusion–reaction equations, this model combines physical and biological processes within a single computational framework to evaluate the system's thermodynamic efficiency, biomass dynamics, and economic feasibility. The results show that with a depth difference of 40 m and a flow rate of 600 kg/s, approximately 9.96 GWh of energy can be produced annually, with a LCOE of 0.03 USD/kWh and a positive net present value (NPV ≈ 6.8 million USD). Furthermore, it was determined that the system could reduce carbon emissions by up to 4,682 tons of CO_2 per year and contribute to eutrophication control through nutrient removal. In this regard, the study presents an applicable model for sustainable coastal development within the scope of blue growth strategies by bringing together energy, food, and environmental components on a single integrated platform.

Keywords: *Ocean thermal energy conversion (OTEC); integrated multi-trophic aquaculture (IMTA); bioremediation; anemone-zooxanthellae; organic Rankine cycle (ORC); sustainable coastal management.*

1. Introduction

Global climate change and energy security concerns have intensified the need to explore renewable energy sources, including ocean-based technologies. Among these, Ocean Thermal Energy Conversion (OTEC) is particularly promising due to its ability to generate continuous, 24/7 power by exploiting the temperature gradient between surface and deep seawater [1-4]. Nevertheless, the economic viability of OTEC systems typically requires a temperature difference exceeding 20 ºC, which restricts their applicability in temperate regions such as Türkiye [5-7]. This study investigates the hypothesis that this limitation can be addressed through the integration of Organic Rankine Cycle (ORC) technologies, which are capable of operating efficiently at lower temperature differentials ($\Delta T \approx 10 - 15°C$) [8, 9].

ORC utilizes organic working fluids with low boiling points such as refrigerants or hydrocarbons in lieu of water, enabling operation under relatively low temperature conditions [10]. This allows for efficient electricity generation even from sources with low temperatures, such as 80-90°C. In OTEC, this technology is optimized to operate at much lower temperature differences, such as 10-15°C [8, 11].

The most critical factor for efficiency is the thermodynamic properties of the working fluid. For low ΔT applications, fluids that vaporize at low pressure at surface water temperatures (e.g., 25-28°C) and condense easily at deep water temperatures (e.g., 12-15°C) are required [8]. Fluids such as ammonia (NH_3) [12], R134a [13], R245fa [14], and R290 [15] have been extensively studied in the literature. Ammonia, in particular, is one of the most preferred fluids for OTEC due to its high heat transfer coefficient [9, 10]. Components can be added to the cycle to increase its low efficiency. Massive heat exchangers (evaporator and condenser) account for approximately 30-50% of OTEC's capital expenditure (CapEx) [3, 6]. Low ΔT requires very large surface areas for heat transfer. Therefore, intensive research is being conducted on compact and highly efficient heat exchanger designs (plate, shell-and-tube, etc.). Although corrosion and biofouling-resistant materials such as titanium are used, this increases the cost [16].

The world's first grid-connected OTEC plant was established in Hawaii, USA. This 105 kW plant operates

*Corresponding Author

with a temperature difference of approximately 20°C and uses an ammonia-based closed-cycle ORC system [17, 18]. This facility is one of the most important references proving the technology's applicability. The facility in Kumejima, Japan, not only produces energy but also offers an integrated model by utilizing OTEC by-products (deep seawater) [19]. Deep seawater is used for aquaculture (shrimp, seaweed), agriculture (sea grapes), drinking water, and cosmetics production.

Simultaneously, intensive fish farming activities cause eutrophication and water quality degradation by loading coastal ecosystems with high amounts of nitrogen and phosphorus through feed residues and metabolic waste. Integrated Multi-Trophic Aquaculture (IMTA) systems developed to address this problem aim to create ecological cycles by converting the waste of one species into a food source for another [20]. The basic philosophy of IMTA is that the waste of one species (e.g., fish feces and feed residues) is a food source for another species. Inorganic waste (ammonia, nitrate, phosphate) released from fish farms is an excellent fertilizer source for zooxanthellae, the symbiotic algae of anemones. Zooxanthellae use these nutrients to perform photosynthesis, cleaning the water in the process and releasing dissolved oxygen into the water, which is vital for fish [21- 25].

Fish farms can cause eutrophication (excessive nutrient accumulation), which is a serious threat to the surrounding ecosystem [26]. Laboratory studies have also demonstrated that cnidarians such as anemones and corals similarly consume ammonia and nitrate efficiently, thereby significantly improving local water quality. Research on coral reefs shows how corals (organisms belonging to the same phylum as anemones and harboring zooxanthellae) efficiently recycle nutrients in their environment [27, 28]. Improved water quality and oxygen levels in IMTA systems allow fish to grow in a less stressful environment. This increases resistance to disease and reduces treatment costs. More importantly, healthier fish use feed more efficiently. This lowers the Feed Conversion Ratio (FCR). Even a small decrease in FCR (e.g., from 1.5 to 1.4) translates to significant savings in feed costs, the largest expense in fish farming [20]. While previous studies have focused on OTEC integration with traditional IMTA components like seaweed and mussels, the use of the anemone–zooxanthellae symbiotic system as a dedicated bioremediation module coupled with OTEC has not yet been investigated, representing a significant gap this study aims to fill.

This study opens a new door in the literature by combining these two concepts. In the proposed system, OTEC not only produces clean energy but also directs nutrient-rich deep seawater and nutrient-rich water from the fish farm to the anemone-zooxanthellae system, which acts as a bioreactor. This symbiotic system purifies the water by efficiently consuming inorganic nutrients in the wastewater while returning dissolved oxygen, critical for fish health, to the environment through photosynthesis. The main objective of this study is to investigate the technical, ecological, and economic feasibility of this synergistic integration for Turkiye's southeastern Aegean coast through a numerical model.

2. Methodology

This study is based on a numerical modeling approach developed to evaluate the performance of a conceptual system.

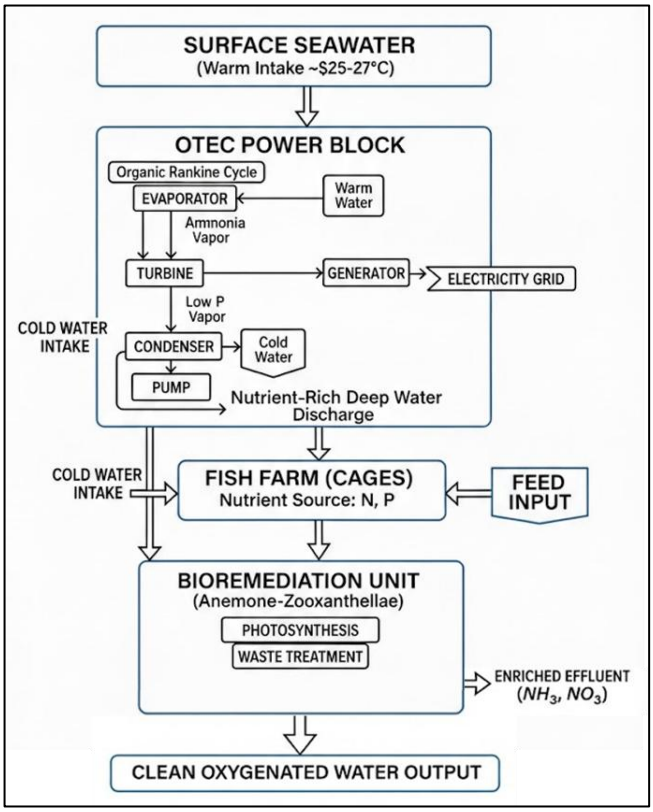


Figure 1. Conceptual engineering schematic of the OTEC-assisted integrated mariculture system.

The thermodynamic and biological performance of the system was modeled using a quasi-steady-state numerical approach implemented in MATLAB [29]. The simulation employs a fixed-point iteration algorithm to solve the coupled mass and energy balance equations across monthly time steps. Ammonia was assumed as the working fluid for the ORC due to its superior thermodynamic properties and heat transfer coefficients at the low temperature differentials characteristic of the study region. To solve the governing Advection-Diffusion-Reaction (ADR) equation, the spatial domain was discretized using a finite difference scheme with a spatial resolution of $\Delta x=1$ m. The temporal evolution was computed using a semi-implicit time-stepping method to ensure numerical stability. The coupling between the thermodynamic (OTEC) and biological modules was handled via a sequential iterational loop in MATLAB, where the output temperature and flow rate of the OTEC block served as boundary conditions for the biological flux inputs. Convergence was assumed when the residuals for nutrient concentration and biomass density fell below 10^{-6}.

The model consists of three main subsystems:

i. An OTEC power block with a closed-loop ORC unit,
ii. A fish cage system defined as a nutrient source,
iii. An anemone-zooxanthellae bioremediation unit positioned downstream of the fish cages.

The OTEC system uses surface warm water (approximately 25-27°C) to vaporize an organic fluid, turn the turbine, and then completes the cycle by condensing it with cold water drawn from the depths (approximately 13-15°C) [8, 30, 31]. The ammonia- and nitrate-enriched water discharged from the fish cage is directed to the area where the anemones are located. Here, the zooxanthellae algae living in the anemone tissue perform photosynthesis using these nutrients and sunlight.

The system (Figure 1) operates on a cascading principle: (1) Energy Generation: Warm surface water drives the

Organic Rankine Cycle (ORC) evaporator, while cold deep water (pumped from depth) acts as the heat sink in the condenser. (2) Nutrient Injection: The nutrient-rich deep water, after leaving the OTEC condenser, is mixed into the mariculture zone, potentially upwelling nutrients. (3) Bioremediation: The effluent from the fish farm, laden with metabolic waste (ammonia/nitrates), flows downstream to the symbiotic anemone-zooxanthellae unit. This unit utilizes solar irradiance and inorganic nutrients to produce biomass and oxygen, closing the ecological loop.

The model was fed with data obtained from the literature, meteorological measurement reports [30], and satellite data [31] for the Datça-Gökova line, which is the working area. These data include monthly average surface and deep water temperatures (Table 1) [30, 31], current velocities, sunshine duration (PAR), water optical properties, and biological kinetic coefficients (Table 2) [11, 12, 16, 17, 19, 20, 26].

Table 1. Monthly Average Surface and Deep Water Temperatures (°C) (Data averaged over the 2018–2023 period).

Month	Surface Water Temperature (SST, 0-5 m)	Deep Water Temperature (100-300 m)
January	16.5	14.5
February	15.8	14.2
March	16.2	14.0
April	17.5	13.8
May	20.0	13.6
June	23.5	13.5
July	26.0	13.5
August	27.2	13.5
September	25.8	13.6
October	23.0	13.8
November	20.5	14.0
December	18.0	14.2

Table 2. Data Used in The Model.

Parameter	Value - Range
Sea water specific heat	3950 J/kgK
Deep water mass flow rate	200 – 800 kg/s
OTEC/ORC efficiency	0.08 – 0.12
Initial biomass	50 – 200 mg/m^3
Maximum growth rate	0.6 – 1.2 1/day
Monod constant	0.01 – 0.05 mg/l
Nutrient consumption coefficient	0.07 – 0.1 mg N / mg Biomass
Q10 temperature factor	2 – 2.2
Reference temperature	25 ºC
Average current speed	0.05 – 0.1 m/s
Effective diffusion coefficient	1 – 10 m^2/s
Model length (x-direction)	100 m
Average light intensity (PAR)	800 – 1500 µmol photon / m^{2}s
Optimal light value	400 – 600 µmol photon / m^{2}s
Sunshine duration	8 – 14 hours/day

The dynamics were modeled based on the advection-diffusion-reaction (ADR) equation (Eq. (1)) [32].

$$\frac{\partial C}{\partial t} + u\frac{\partial C}{\partial x} = D\frac{\partial^2 C}{\partial x^2} + S \tag{1}$$

This equation simulates the temporal and spatial changes of the fundamental variables in the model area (ammonia concentration, dissolved oxygen, zooxanthellae biomass), their transport by currents (advection), turbulent mixing (diffusion), and biochemical transformations (reaction).

Biomass growth kinetics are formulated using the Monod (Eqs. (2-4)) and Steele (Eq. (5)) equations, which consider nutrient and light limitations, while temperature dependence is formulated using the Q10 factor (Eq. (6)) [33, 34].

$$\mu = \mu_{max}\frac{C_N}{K_S + C_N} f_l(l) f_T(T) \tag{2}$$

$$R_{cons} = \frac{\mu B}{Y_{N/B}} \tag{3}$$

$$R_{O_2} = \mu B Y_{O_2} \tag{4}$$

$$f_I(l) = \frac{l}{l_{opt}} e^{1-\frac{l}{l_{opt}}} \tag{5}$$

$$f_T(T) = Q_{10}^{\left(\frac{T-T_{ref}}{10}\right)} \tag{6}$$

The OTEC power generation calculation is based on engineering parameters such as thermodynamic cycle efficiency, heat exchanger performance, and parasitic pump loads (Eqs. (7-10)) [35].

$$\eta_{Carnot} = 1 - \frac{T_c}{T_h} \tag{7}$$

$$P_{gross} = \dot{m}_h c_p (T_{h,in} - T_{h,out}) \eta_{ORC} \tag{8}$$

$$P_{pump} = \frac{\dot{m}_c g H}{\eta_{pump}} \tag{9}$$

$$P_{net} = P_{gross} - P_{pump} \tag{10}$$

Here, H is the total dynamic head, which accounts for both the vertical depth difference between the warm and cold water intakes and all frictional pressure losses in the piping and heat exchangers. It is crucial to distinguish between the physical cold water intake depth and the hydraulic parameter used in the pump power calculation. While the cold seawater is physically extracted from depths exceeding 150–300 m, the modeled parameter $H = 40\,m$ represents the Total Dynamic Head (TDH). This value accounts for the cumulative friction losses in the heat exchangers and piping, as well as the static lift required for the pumping system, rather than the vertical depth of the resource.

Eqs. (11) and (12) are used to assess the economic feasibility and environmental benefits of the study [36].

$$LCOE = \frac{CapEx\,\frac{r(1+r)^N}{(1+r)^N - 1} + OpEx}{E_{annual}} \tag{11}$$

$$CO_2^{eq,avoided} = E_{annual}\left(EF_{grid} - EF_{OTEC}\right) \tag{12}$$

The economic feasibility analysis is grounded in specific financial assumptions derived from small-to-medium scale marine renewable installations. Based on the simulation parameters, the baseline scenario assumes a Capital

Expenditure (CapEx) of 2.5 million USD and an annual Operational Expenditure (OpEx) of 50000 USD [5, 7, 8]. The financial projection is calculated over a project lifetime of 20 years with a discount rate (r) of 8%. These values were selected to reflect the shared infrastructure costs inherent in an integrated mariculture-energy platform. This calculation assumes a grid emission factor (EF_{grid}) of 0.5 kg CO_2/kWh compared to the OTEC system's minimal footprint (EF_{OTEC}) of 0.03 kg CO_2/kWh.

3. Results and Discussion

The operational parameters for the main scenario were selected considering the specific hydrographic constraints of the Datça-Gökova coastline. Bathymetric data indicates that the required depth for cold water intake ($300 + m$) is accessible within a distance of 2–3 km from the shore in this region, which technically justifies the modeled pipe lengths and associated friction head losses. Furthermore, the mass flow rate range aligns with the intake capacities of pilot-scale OTEC plants operating in similar shelf environments, ensuring the scenario remains within practical engineering limits. Under the model's main scenario conditions ($H = 40\,m, \dot{m} = 600\,kg/s, \eta_{ORC} = 0.08$), the annual energy production was calculated to be approximately 9.96 GWh, with an average net power of 1130.85 kW. In this case, the pump power remained at 276.99 kW, the system's LCOE value was found to be 0.0306 USD/kWh, and the net present value (NPV) was 6.79 million USD. The calculated LCOE value is consistent with the range of 0.03–0.07 USD/kWh reported in the literature for small-to-medium-scale OTEC systems recommended for tropical and subtropical regions [3, 8]. This result indicates that OTEC-based systems may be economically viable for mariculture applications. It should be emphasized that the reported LCOE and NPV values correspond to an optimistic, site-specific scenario reflecting favorable bathymetry, short intake distances, and shared infrastructure with mariculture facilities. These economic indicators should therefore be interpreted as representative upper-bound performance estimates rather than universally achievable values for standalone OTEC installations. It is important to emphasize that these findings represent an optimistic, site-specific scenario. While the integrated nature of the system reduces costs through shared infrastructure, standalone OTEC applications in less favorable bathymetric conditions or without cost-sharing would likely result in higher LCOE values.

The calculated LCOE of approximately 0.03 USD/kWh is notably lower than standalone OTEC pilot projects reported in the literature. While large-scale OTEC estimations often project LCOE values between 0.15–0.20 USD/kWh, the significantly lower value obtained in this study is consistent with recent findings on multipurpose OTEC systems, where cost-sharing with secondary industries (aquaculture, desalination) can reduce effective energy costs by up to 60%. This reduction is primarily attributed to the synergistic cost-sharing nature of the proposed integrated system. By co-locating with the aquaculture facility, the OTEC unit utilizes shared mooring systems, platform infrastructure, and logistical support, effectively distributing the capital burden. Furthermore, the exclusion of dedicated deep-water pipe costs—assuming integration with existing mariculture water intake infrastructure—significantly lowers the effective CapEx attributed solely to power generation.

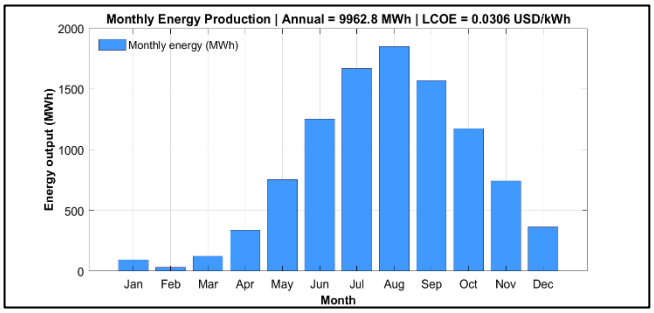


Figure 2. Monthly energy outlook.

Figure 2 shows the variation in annual energy production and LCOE values. It can be seen that power production increases non-linearly with increasing depth difference (ΔT) and flow rate, while LCOE values decrease significantly. This indicates that the system's optimal operating region, both thermodynamically and economically, is at medium-high flow rates (600–1200 kg/s) and a cycle efficiency of 0.08–0.1.

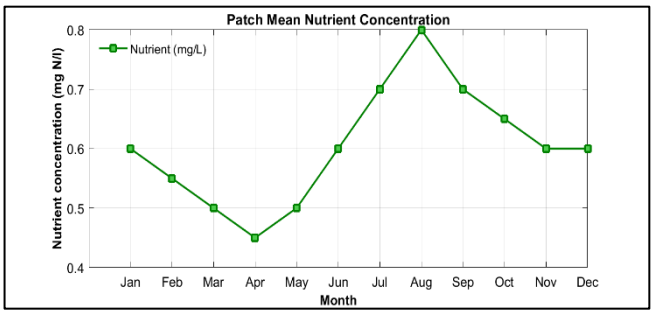


Figure 3. Patch mean nutrient concentration.

Figure 3 shows the monthly variation in nutrient concentrations. While nutrient concentrations range from 0.45 to 0.6 mg/l during the winter months, they increase to levels of 0.7–0.8 mg/l during the summer months. This increase indicates that the OTEC system's deep water supply can transport additional nutrients to the surface ecosystem and that biomass growth (B) accelerates during the summer period. The model's biological module (Monod + Steele-type light limitation) confirmed this trend; Figure 4 shows that both temperature and biomass increase simultaneously peak during the summer months.

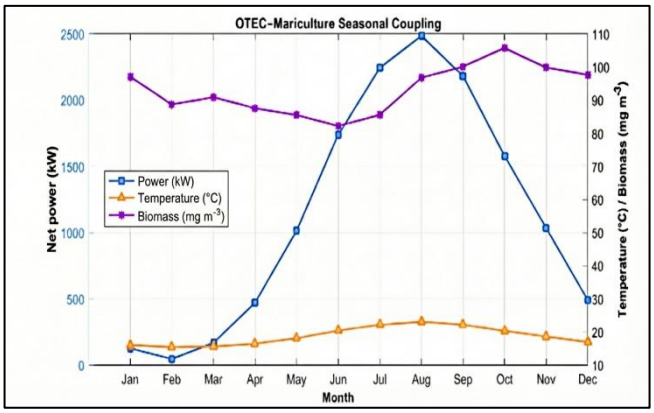


Figure 4. OTEC-Mariculture seasonal coupling.

Figure 4 compares power production, patch temperature, and biomass concentration on a monthly basis. Power production reached 2–2.5 MW during July–September, while patch temperature stabilized around 26–27 °C. During the same period, biomass concentration increased to 100–

106 mg/m^3. These findings indicate that the OTEC-supported water column mixture can support mariculture production by maintaining thermal and nutritional balance.

The bioremediation module demonstrates a quantifiable ecosystem service driven by the nitrogen-to-biomass conversion coefficient ($Y_{N/B} = 0.1$). The numerical model indicates that the anemone-zooxanthellae patch acts as a net nutrient sink. Under the simulated growth kinetics ($\mu_{max} = 0.05\ d^{-1}$), the system actively consumes dissolved inorganic nitrogen from the aquaculture effluent, thereby reducing the local nutrient load and mitigating eutrophication risks associated with intensive fish farming. Quantitatively, the simulation results demonstrated that the integrated anemone-zooxanthellae system is capable of removing approximately 24.5% of the total inorganic nitrogen load discharged from the fish cages during the peak summer growth period. This corresponds to an annual removal of roughly 315 kg of nitrogen, directly converting waste into harvestable biomass. From an IMTA perspective, the modeled nitrogen removal efficiency is consistent with values reported for extractive components such as macroalgae and bivalves, which typically exhibit nitrogen uptake efficiencies ranging from low double-digit percentages to approximately 30% depending on species, hydrodynamic conditions, and nutrient loading. Qualitatively, this 24.5% removal efficiency is comparable to reported nitrogen uptake rates in seaweed-based IMTA systems, which typically range from 15% to 40% depending on the species [20] and hydrodynamic conditions. This suggests that the symbiotic anemone-zooxanthellae module can serve as an effective biological filter within the established ecological range of traditional extractive organisms. While the present system operates under simplified numerical assumptions, the obtained removal magnitude indicates that the anemone–zooxanthellae module performs within the expected ecological efficiency envelope of established IMTA configurations.

A sensitivity analysis was conducted to evaluate the robustness of the economic indicators against parameter uncertainties. Three alternative scenarios were tested against the base case (A_0) doubling the capital cost (A_1), reducing the mass flow rate (A_2), and improved efficiency (A_3). Results indicate that LCOE is most sensitive to initial capital costs, rising to ~0.056 USD/kWh under the doubled CapEx scenario. However, even under these conservative conditions, the system maintains a positive NPV, confirming its financial viability.

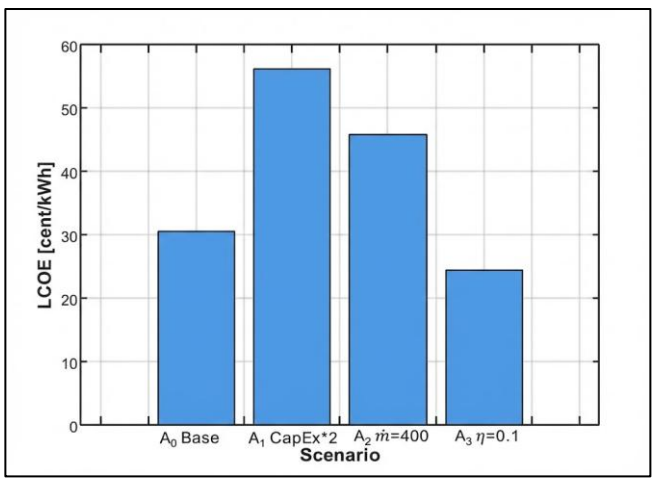


Figure 5. LCOE variation according to different scenarios.

Figure 5 shows the distribution of annual energy production and LCOE for different flow rate and cycle efficiency combinations of the system. The graph shows that LCOE is high (0.08–0.1 USD/kWh) with low NPV (approximately 0–2 million USD) in base scenarios, while in high efficiency–high flow rate combinations, LCOE falls below 0.01 USD/kWh under aggressive scaling scenarios, and NPV reaches 30–40 million USD levels. This trend confirms the system's scale-up potential.

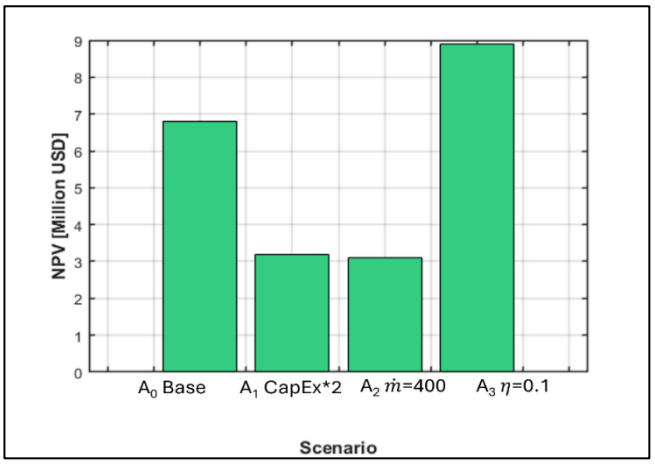


Figure 6. NPV variation according to different scenarios.

Figure 6 shows the effect of economic parameters (CapEx and OpEx). It is seen that when CapEx is doubled, LCOE increases by approximately 80%, but energy production remains constant. In contrast, under the same conditions, the NPV value is calculated to decrease from USD 6.8 million to USD 3.2 million. This result clearly demonstrates the critical role of investment costs in economic feasibility. However, the fact that operational costs (OpEx) remain proportional to annual energy production indicates that the system remains sustainable in terms of maintenance and operation.

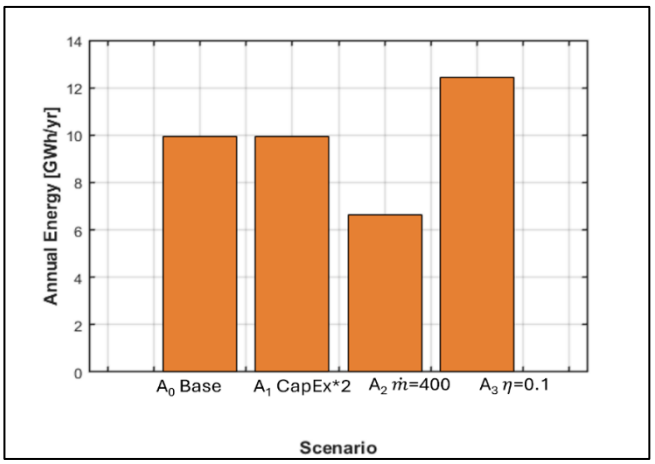


Figure 7. Annual energy variation according to different scenarios.

Figure 7 shows the relationship between annual energy production and net present value. The linear-like trend obtained indicates that a 10% increase in energy production raises the NPV by approximately USD 1.2 million. This reveals that the model directly translates energy performance into economic returns and that improving system efficiency significantly shortens the investment payback period.

Overall, when Figures 5–7 are evaluated together, it can be said that the model provides consistent results both technically and economically. The relationship between LCOE, NPV, and energy production is consistent with other OTEC economic assessments in the literature [12, 16] and clearly indicates which parameters will be decisive in the system's transition to commercial scale.

Environmental impact assessment reveals a significant decarbonization potential. Based on the model's annual energy production of approximately 9.96 GWh and a net emission reduction factor, the system mitigates approximately 4,682 tons of CO_2 equivalent per year.

In conclusion, the model outputs were found to be thermodynamically, economically, and ecologically consistent with each other. A positive correlation was found between power production and biological production potential. The parameter ranges are consistent with the data from OTEC pilot plants [8, 9] in the current literature, and no extreme or physically impossible values were reached.

3.1. Limitations, Engineering Challenges, and Future Work

The present model provides a robust theoretical foundation; however, the transition to commercial scale involves significant engineering and regulatory challenges. A critical factor is the long-term performance of the heat exchangers, particularly the risk of biofouling and corrosion, which are only briefly mentioned in the Introduction. Future work must incorporate fouling mitigation strategies (e.g., automated cleaning systems or biocide injection) and their associated operating costs into the economic model. Furthermore, the potential environmental impact of discharging large volumes of cold, nutrient-rich deep water near the surface ecosystem needs to be studied using high-resolution 3D hydrodynamic models. Regulatory frameworks for co-locating OTEC and IMTA are also nascent and require proactive development to streamline permitting.

4. Conclusions

This study presents a numerical investigation offering a theoretical framework of the theoretical feasibility of an integrated OTEC-assisted mariculture and bioremediation concept for sustainable coastal development. This approach, which combines energy production, waste management, and food production within a single circular system, enables the reduction of environmental impacts while also facilitating the development of economically viable new business models. The model serves as an important reference for blue growth strategies in regions with similar thermal and ecological characteristics, particularly along the Türkiye's coastal regions.

The analysis results show that the system, operating at a depth difference of 40 m and a flow rate of 600 kg/s, can produce approximately 9.96 GWh of energy annually and can be economically competitive with an LCOE of 0.0306 USD/kWh. The thermodynamic and economic performance of the model is consistent with the literature, achieving a stable balance in terms of both energy production and biological growth.

The presented model extends the traditional IMTA concept by introducing a new harvestable product chain. Anemones have economic value in the aquarium sector, and the potential use of bioactive compounds that can be obtained from zooxanthellae adds diversity to the study's revenue model.

Despite the marginal temperature difference at the study location, the integration of ORC technology proved technically feasible for maintaining continuous power generation. Consequently, minimizing the initial investment costs (CapEx) remains the primary factor for enhancing economic competitiveness.

In conclusion, this model offers not only an energy production concept but also a comprehensive framework for sustainable marine resource management, waste recovery, and food security. It is important to note that the presented findings are derived from a numerical modeling framework and have not yet been validated through pilot-scale or operational deployments. Consequently, the results should be interpreted as indicative performance trends rather than definitive operational benchmarks. Within these limitations, OTEC-supported mariculture systems have the potential to become one of the fundamental components of future carbon-neutral coastal economies.

While the numerical model provides encouraging results, these findings should be treated as indicative performance trends. Future experimental validation and pilot-scale operations are necessary to transition from this theoretical case study to a fully operational system.

Conflict of Interest

The author declares no conflict of interest.

Credit Author Statement

M. Ökten: Conceptualization, Data curation, Methodology, Validation, Visualization, Writing- Original draft preparation, Writing- Reviewing and Editing.

Nomenclature

B	Biomass concentration [mg/m^3]
C	Concentration [mg/l]
c	Specific heat [$J/kg \cdot K$]
$CapEx$	Capital cost [$]
D	Effective diffusion coefficient
e	Euler's constant [2.718]
E	Energy [$kWh/year$]
EF	Carbon factor [$kg\ CO_2/kWh$]
f	Function
g	Gravitational acceleration [9.81 m/s^2]
H	Total dynamic (depth + friction losses) head [m]
l	Light intensity [$\mu mol\ photons/m^2 \cdot s$]
$LCOE$	Levelized Cost of Energy [$/$kWh$]
K	Monod constant [mg/l]
m	Meter
$\dot{m}$	Mass flow rate [kg/s]
N	Equipment lifetime [$years$]
NPV	Net Present Value [$]
$OpEx$	Annual operating cost [$/year$]
P	Power [kW]
Q	Temperature factor
r	Discount rate [%]
R	Rate [$mg\ /m^3 \cdot day$]
S	Source/sink term
t	Time [s]
T	Temperature [℃]
u	Velocity [m/s]

x	Distance in the flow direction $[m]$
Y	Coefficient $[mg\ /mg\ biomass]$

Greek symbols

μ	Growth rate $[l/day]$
η	Efficiency

Subscripts

c	Cold
h	Hot
in	Inlet
l	Light
n	Nutrient
N/B	Nitrogen / Biomass
out	Outlet
O_2	Oxygen
p	Pressure

References:

[1] J. Tan *et al.*, "Stability analysis on internal flow-induced cold-water pipe with non-uniform and variable cross-section for OTEC subject to multiple clump weights," *Ocean Engineering*, vol. 330, Art. no. 121191, Jun. 2025, doi: 10.1016/j.oceaneng.2025.121191.

[2] A. M. Faizatama *et al.*, "Hydrodynamic impact of cold-water pipes and mooring systems on KVLCC2 for floating OTEC platforms," *Ocean Engineering*, vol. 341, Dec. 2025, Art. no. 122491, doi: 10.1016/j.oceaneng.2025.122491.

[3] M. S. Calvo and H. S. Lee, "Ocean thermal energy conversion (OTEC) potential in central American and Caribbean regions: A multicriteria analysis for optimal sites," *Applied Energy*, vol. 394, Sep. 2025, Art. no. 126182, doi: 10.1016/j.apenergy.2025.126182.

[4] E. Tang, J. Gao, W. Huang, and Y. Qian, "Marine renewable energy: Progress, challenges, and pathways to scalable sustainability," *Energy*, vol. 335, Oct. 2025, Art. no. 138083, doi: 10.1016/j.energy.2025.138083.

[5] Q. Ma *et al.*, "Innovative design and performance evaluation of a compact 1 MW radial inflow turbine with non-azeotropic fluids for ocean thermal energy conversion applications," *Energy*, vol. 335, Oct. 2025, Art. no. 138105, doi: 10.1016/j.energy.2025.138105.

[6] L. Cheddie, S. Kelly, and D. Balladin, "Utilizing AHP-TOPSIS to select an OTEC cycle type for Tobago," *Renewable Energy*, vol. 257, Feb. 2026, Art. no. 124727, doi: 10.1016/j.renene.2025.124727.

[7] K. Sanjivy et al., "Harnessing the Ocean's depths: SWAC and OTEC for sustainable cooling and power – A review of technologies, applications and challenges," *Renewable and Sustainable Energy Reviews*, vol. 226, Part A, Jan. 2026, Art. no. 116253, doi: 10.1016/j.rser.2025.116253.

[8] P. Lykas et al., "Energy, exergy, and economic comparison of ORC with quasi-isothermal expansion with other ORC designs for low-grade waste heat recovery," *Thermal Science and Engineering Progress*, vol. 55, Oct. 2024, Art. no. 103010, doi: 10.1016/j.tsep.2024.103010.

[9] D. Gonidaki, E. Bellos, and K.-S. Nikas, "Comparative thermodynamic analysis of Kalina cycle and ORC configurations for the utilization of low to high grade geothermal sources," *Applied Thermal Engineering*, vol. 283, Jan. 2026, Art. no. 129006, doi: 10.1016/j.applthermaleng.2025.129006.

[10] B. F. Tchanche, Gr. Lambrinos, A. Frangoudakis, and G. Papadakis, "Low-grade heat conversion into power using organic Rankine cycles – A review of various applications," *Renewable and Sustainable Energy Reviews*, vol. 15, no. 8, pp. 3963–3979, Oct. 2011, doi: 10.1016/j.rser.2011.07.024.

[11] C. G. F. Do Val, J. A. M. Silva, and S. Oliveira Jr., "Deep Water Cooled ORC for Offshore Floating Oil Platform Applications," *International Journal of Thermodynamics*, vol. 20, no. 4, pp. 229–237, 2017, doi: 10.5541/eoguijt.359499.

[12] H. Uehara, A. Miyara, Y. Ikegami, and T. Nakaoka, "Performance Analysis of an OTEC Plant and a Desalination Plant Using an Integrated Hybrid Cycle," *Journal of Solar Energy Engineering*, vol. 118, no. 2, pp. 115–122, May 1996, doi: 10.1115/1.2847976.

[13] M. Hijriawan, N. A. Pambudi, D. S. Wijayanto, M. K. Biddinika, and L. H. Saw, "Experimental analysis of R134a working fluid on Organic Rankine Cycle (ORC) systems with scroll-expander," *Engineering Science and Technology, an International Journal*, vol. 29, May 2022, Art. no. 101036, doi: 10.1016/j.jestch.2021.06.016.

[14] R. Kong, T. Deethayat, A. Asanakham, N. Vorayos, and T. Kiatsiriroat, "Thermodynamic performance analysis of a R245fa organic Rankine cycle (ORC) with different kinds of heat sources at evaporator," *Case Studies in Thermal Engineering*, vol. 13, Mar. 2019, Art. no. 100385, doi: 10.1016/j.csite.2018.100385.

[15] W. Gao, Z. Wu, Z. Tian, and Y. Zhang, "Experimental investigation on an R290-based organic Rankine cycle utilizing cold energy of liquid nitrogen," *Applied Thermal Engineering*, vol. 202, Feb. 2022, Art. no. 117757, doi: 10.1016/j.applthermaleng.2021.117757.

[16] B. Martin, S. Okamura, T. Yasunaga, Y. Ikegami, and N. Ota, "OTEC and Advanced Deep Ocean Water Use for Kumejima: An Introduction," in *Proceedings IEEE OCEANS Chennai*, Feb. 2022, pp. 1–5, doi: 10.1109/OCEANSChennai45887.2022.9775240.

[17] "Makai's Ocean Thermal Energy Conversion (OTEC) Power Plant, Hawaii," Power Technology. Accessed: Jun. 26, 2020. [Online]. Available: https://www.power-technology.com/projects/makais-ocean-thermal-energy-conversion-otec-power-plant-hawaii/

[18] K. Park, Z. Yang, A. E. Copping, and F. T. Rollano, "A modeling study of ocean thermal energy conversion resource and potential environmental effects around Kailua-Kona, Hawaii," *Renewable Energy*, vol. 253, Nov. 2025, Art. no. 123616, doi: 10.1016/j.renene.2025.123616.

[19] "Okinawa OTEC Demonstration Facility." Accessed: Oct. 19, 2025. [Online]. Available: http://otecokinawa.com/en/

[20] M. Troell, A. Joyce, T. Chopin, A. Neori, A. Buschmann, and J.-G. Fang, "Ecological Engineering in

Aquaculture – Potential for Integrated Multi-Trophic Aquaculture (IMTA) in Marine Offshore Systems," *Aquaculture*, vol. 297, pp. 1–9, Dec. 2009, doi: 10.1016/j.aquaculture.2009.09.010.

[21] B. Quinn, F. Gagné, and C. Blaise, "An investigation into the acute and chronic toxicity of eleven pharmaceuticals (and their solvents) found in wastewater effluent on the cnidarian, Hydra attenuata," *Science of The Total Environment*, vol. 389, no. 2–3, Jan. 2008, pp. 306–314, doi: 10.1016/j.scitotenv.2007.08.038.

[22] R. Devereux, M. G. J. Hartl, M. Bell, and A. Capper, "The abundance of microplastics in cnidaria and ctenophora in the North Sea," *Marine Pollution Bulletin*, vol. 173, Part A, 2021, Art. no. 112992, doi: 10.1016/j.marpolbul.2021.112992.

[23] M. Amin et al., "Decontamination of industrial wastewater using microalgae integrated with biotransformation of the biomass to green products," *Energy Nexus*, vol. 6, 2022, Art. no. 100089, doi: 10.1016/j.nexus.2022.100089.

[24] I. Hamid and W. A. Khanday, "Recent advances in antibiotic removal methods from wastewater: A comprehensive review," *Separation and Purification Technology*, vol. 381, 2026, Art. no. 135478, doi: 10.1016/j.seppur.2025.135478.

[25] P. Hu et al., "Nutrient removal and metabolic adaptation in Mercenaria mercenaria during aquaculture wastewater bioremediation," *Aquaculture*, vol. 611, Jan. 2026, Art. no. 743049, doi: 10.1016/j.aquaculture.2025.743049.

[26] T. Chopin, J. Cooper, G. K. Reid, S. Cross, and C. Moore, "Open-water Integrated Multi-Trophic Aquaculture: environmental biomitigation and economic diversification of fed aquaculture by extractive aquaculture," *Reviews in Aquaculture*, vol. 4, pp. 209–220, Dec. 2012, doi: 10.1111/j.1753-5131.2012.01074.x.

[27] S. Davy and C. B. Cook, "The relationship between nutritional status and carbon flux in the zooxanthellate sea anemone Aiptasia pallida," *Marine Biology*, vol. 139, pp. 999–1005, Nov. 2001, doi: 10.1007/s002270100640.

[28] "Cooke Seafood » Sustainability." Accessed: Oct. 19, 2025. [Online]. Available: https://cookeseafood.com/sustainability/

[29] MATLAB, *version 9.13.0 (R2022b)*. Natick, Massachusetts: The MathWorks Inc., 2022.

[30] "Turkish State Meteorological Service Official Web Sites." Accessed: Oct. 19, 2025. [Online]. Available: https://www.mgm.gov.tr/eng/forecast-cities.aspx

[31] "Home | CMEMS." Accessed: Oct. 19, 2025. [Online]. Available: https://marine.copernicus.eu/

[32] B. M. Gillanders, T. S. Elsdon, and M. Roughan, "Connectivity of Estuaries," in *Treatise on Estuarine and Coastal Science*, E. Wolanski and D. McLusky, Eds., Academic Press, 2011, pp. 119–142, doi: 10.1016/B978-0-12-374711-2.00709-9.

[33] H. El Bari, M. Bakraoui, Y. El Gnaoui, and F. Karouach, "Kinetics models of methane production from anaerobic digestion," in *Clean Energy and Resources Recovery*, V. Tyagi and K. Aboudi, Eds., Elsevier, 2021, pp. 271–294, doi: 10.1016/B978-0-323-85223-4.00020-8.

[34] C. Cobelli, A. Mari, and E. Ferrannini, "Non-steady state: Error analysis of Steele's model and developments for glucose kinetics," *American Journal of Physiology*, vol. 252, no. 5, pp. E679–E689, May 1987, doi: 10.1152/ajpendo.1987.252.5.E679.

[35] W. Liu *et al.*, "A review of research on the closed thermodynamic cycles of ocean thermal energy conversion," *Renewable and Sustainable Energy Reviews*, vol. 119, p. 109581, Mar. 2020, doi: 10.1016/j.rser.2019.109581.

[36] C. Lucheroni and C. Mari, "CO2 volatility impact on energy portfolio choice: A fully stochastic LCOE theory analysis," *Applied Energy*, vol. 190, pp. 278–290, Mar. 2017, doi: 10.1016/j.apenergy.2016.12.125.